A polynomial hybrid reflection model and measurement of its parameters based on images of sample

Lei Yang (杨 磊) and Jiuqiang Han (韩九强)

School of Electronics and Information Engineering, Xi'an Jiaotong University, Xi'an 710049

Received April 27, 2007

Reflectance model is a basic concept in computer vision. Some existing models combining the classical diffuse reflectance model and those for surfaces containing specular components can approximately describe real reflectance. But the ratio of diffuse and specular reflection decided manually has no clear meaning. We propose a new polynomial hybrid reflectance model. The reflectance map equation with a known shape (for example cylinder) as a sample is used to estimate parameters of the proposed reflectance model by least square regression algorithm. Then the reflectance parameters for surfaces of the same class of materials can be determined. Experiments are performed for a metal surface. The synthesis images produced by the proposed method and existing ones are compared with the real acquired image, and the results show that the proposed reflectance model is suitable for describing real reflectance.

OCIS codes: 100.2960, 120.5820, 160.4760, 290.5820, 290.5880.

Reflectance model is an important concept in computer vision[1]. Using the conception of reflectance model, the procedure of imaging can be simulated. The brightness of image pixel points is associated with properties of light source, attributes of camera, the orientation (shape) of object, and reflectance properties of the surface[2]. Physical and geometrical optics are two approaches to the study of reflectance[3]. Geometrical models process simpler mathematical forms than physical ones, which makes them more useful. In general, geometrical models are applicable only when the wavelength of incident light is much smaller compared with the dimensions of the surface. A few papers investigate the unified reflectance models from both physical and geometrical optics[4−6]. At early time, Lambertian model was adopted by computer vision due to its simple form[7]. Real materials surfaces show heavy specular component namely highlight, so specular reflectance models are used[8]. But real surface contains both diffuse and specular components. So lots of hybrid reflectance models were proposed[5,9,10], most of which used a linear combination of diffuse and specular reflectance models and isotropic property. However, there is no general reflectance model containing all reflectance properties. On the other hand, the measurement of the reflectance models is still a problem. Gonioreflectometer was used to measure the parameters[5]. But the apparatus for measuring the parameters of reflectance are relative expensive. The measuring methodology based on images is usually chosen[11,12]. Recently, linear subspace was used to investigate Lambertian reflectance and image formation was considered as the analog of convolution[13]. How to express reflectance function was investigated[14], a data-driven reflectance model was also brought forward[15].

We think that the diffuse and specular reflectance properties are distinguished but associated with each other for an object. The image intensity based on diffuse reflectance model is the inner multiplication of vectors of the light source direction and surface normal. The specular image intensity is exponential (or n-order polynomial) of the inner multiplication of the specular direction and surface normal. Using principal direction determined by light direction and specular direction, a mathematical refined m-lobed reflection model was derived in Ref. [9]. The value of weighting factor was gained empirically for the linear combination hybrid model of diffuse and specular models[2]. Based on the reflectance morphology of rough surface[3,9], and inspired by the form of diffuse and specular reflectance models, a new general polynomial hybrid reflectance model is proposed in this paper. The coefficients of the polynomial reflectance model can be estimated using image with known shape by least square regression algorithm. Then the reflectance models for a class of surfaces of the same material can be acquired. Additionally, the proposed method has the following characteristics. 1) Polynomial reflectance models contain wide surface from diffuse to high specular ones (the former is lower-order item and the latter is higher-order item). 2) The reflectance map does not need to be normalized because the irradiance is merged in the coefficients of reflectance model.

Intensities of image are determined by several parameters: location and properties of light, surface properties and orientation $\vec{n}$ of objective in scene, location of camera, and laws of image formation. In shape-from-shading case, we generally assume that the light is a point light source located in infinite position[16,17], its direction is $\vec{n}_\text{i}$ in image center coordinates, and the light strength is E. Observing camera is located in $\vec{n}_\text{o} = (0, 0, -1)$. The radiance of a distant light source can be described by Dirac function as

$$L_\text{i}(\vec{n}) = E\delta(\vec{n} - \vec{n}_\text{o}). \quad (1)$$

The reflected light depends on the radiance of the light and the bidirectional reflection function (BRDF) defined as

$$f(\theta_\text{i}, \phi_\text{i}, \theta_\text{o}, \phi_\text{o}) = \frac{\partial L_\text{o}(\theta_\text{o}, \phi_\text{o})}{\partial L_\text{i}(\theta_\text{i}, \phi_\text{i})}, \quad (2)$$

where $(\theta_\text{i}, \phi_\text{i})$ and $(\theta_\text{o}, \phi_\text{o})$ denote directions of irradiance of incident light L_i and reflected radiance L_o in polar coordinates respectively. With a known BRDF of a surface and a distant point light (assumed in this paper) $E\delta(n-\vec{n}_{\rm o})$, the radiance of reflected light in the viewing direction $\vec{n}$ is

$$L(\vec{n},\vec{n}_{\rm i},\vec{n}_{\rm o}) = \int\limits_{\omega} f(\vec{n},\vec{n}_{\rm i},\vec{n}_{\rm o})L_{\rm i}(\omega){\rm d}\omega$$

$$= f(\vec{n},\vec{n}_{\rm i},\vec{n}_{\rm o})E\max\{0,\vec{n}_{\rm i}^{\rm T}*\vec{n}\}, \quad (3)$$

where the integral domain of ω is hemisphere. The result shows that the intensity I acquired by camera is proportional to $L(\vec{n},\vec{n}_{\rm i},\vec{n}_{\rm o})$, thus we have

$$I(\vec{n},\vec{n}_{\rm i},\vec{n}_{\rm o}) = \alpha L(\vec{n},\vec{n}_{\rm i},\vec{n}_{\rm o}), \quad (4)$$

where α is the proportion constant. Normalized image is used in practice. Let $I_{\max}$ and $I_{\min}$ be the acquired maximum and minimal intensities of image, we get the well-known reflectance map equation,

$$R(\vec{n},\vec{n}_{\rm i},\vec{n}_{\rm o}) = \frac{I(\vec{n},\vec{n}_{\rm i},\vec{n}_{\rm o})-I_{\min}}{I_{\max}-I_{\min}}. \quad (5)$$

From Eq. (3), we find that a right reflectance model can accurately describe the image intensity variation corresponding to the reflection characteristics of the surface. The reflection characteristics of the surface are described by BRDF. Lots of experiential and mathematical reflectance models are formulated from optical radiation[3,6]. Two kinds of extreme reflection models namely diffuse reflection and specular reflection are usually considered in computer vision. The BRDF of Lambertian (diffuse) reflectance model is a constant shown as $f_{\rm d}(\vec{n},\vec{n}_{\rm i},\vec{n}_{\rm o}) = 1/\pi$. In this case, the reflectance map function of the surface illuminated by a point light source is given by

$$R_{\rm d}(\vec{n},\vec{n}_{\rm i},\vec{n}_{\rm o}) = \frac{E}{\pi}\vec{n}^{\rm T}*\vec{n}_{\rm i}. \quad (6)$$

On the other hand, many mathematical reflectance models are used to approximate the characteristic of specular reflection. The ideal specular reflection model is formulated using Dirac function as

$$f_{\rm s}(\vec{n},\vec{n}_{\rm i},\vec{n}_{\rm o}) = \frac{\delta(\vec{n}^{\rm T}*\vec{n}_{\rm spec})}{2\vec{n}^{\rm T}*\vec{n}_{\rm i}}, \quad (7)$$

where the vector $\vec{n}_{\rm spec} = (\vec{n}_{\rm i}+\vec{n}_{\rm o})/\left|\vec{n}_{\rm i}+\vec{n}_{\rm o}\right|$ is called the halfway-vector (or specular reflectance direction) and represents the normalized vector sum between the light source direction and the observing camera direction. Apparently, model (7) cannot be used in practice. A modified Torrance-Sparrow model using a Gaussian distribution to model the facet orientation function is used to deal with specular reflectance phenomena[8]:

$$f_{\rm s}(\vec{n},\vec{n}_{\rm i},\vec{n}_{\rm o}) = \frac{1}{(\vec{n}^{\rm T}*\vec{n}_{\rm i})(\vec{n}^{\rm T}*\vec{n}_{\rm o})}$$

$$\times\exp(-\frac{(\tan\arccos(\vec{n}^{\rm T}*\vec{n}_{\rm spec}))^2}{2\sigma^2}), \quad (8)$$

where the factor σ is the standard deviation, which can be considered as measurement of the surface roughness. In this case, the reflectance map function of the surface is[8]

$$R_{\rm s}(n,\vec{n}_{\rm i},\vec{n}_{\rm o})$$

$$= \frac{E}{(\vec{n}^{\rm T}*\vec{n}_{\rm o})}\exp(-\frac{(\tan\arccos(\vec{n}^{\rm T}*\vec{n}_{\rm spec}))^2}{2\sigma^2}). \quad (9)$$

Another specular model is Phong's model[18] which indicates that the light perceived by the camera is represented as

$$R_{\rm s}(\vec{n},\vec{n}_{\rm i},\vec{n}_{\rm o}) = E(\vec{n}^{\rm T}*\vec{n}_{\rm spec})^k, \quad (10)$$

where k is a constant. Different values of k denote different kinds of surfaces which are more or less mirror-like.

But the surfaces of most real objects are neither purely Lambertian reflectance models, nor purely specular components. Instead, they are a combination of diffuse and specular components. A hybrid model that consists of three components (a diffuse lobe, a specular lobe, and a specular spike) was proposed by Tagare[9]. Based on a set of principal direction $\vec{p}_j$, a general non-Lambertian model is shown as

$$R_{\rm hybrid} = \sum_j \rho_j\Phi(\vec{p}_j^{\rm T}*\vec{n})+b, \quad (11)$$

where ρ_j is albedo, Φ is a monotonically increasing function, and b is a constant. Because $\vec{p}_j$ is derived by the directions of light source vector and observing camera vector, the model (11) can be considered as a function of these vectors. A linear combination model of diffuse and specular components presented by Cho[2] is described as

$$R_{\rm hybrid} = (1-w)R_{\rm d}+wR_{\rm s}, \quad (12)$$

where $R_{\rm hybrid}$ is the total intensity of the surface, $R_{\rm d}$ and $R_{\rm s}$ are the diffuse intensity and the specular intensity, respectively, and w is the weight of the specular component determined empirically.

Inspired by the reflectance models (9) – (11), a new multi-order specular reflectance model based on polynomial of inner multiplications of halfway-vector and surface normals is proposed as

$$R_{\rm s} = E\sum_{k=1}^{\infty}c_k(\vec{n}^{\rm T}*\vec{n}_{\rm spec})^k, \quad (13)$$

where k denotes the kth order mirror-like component, and a series of constants c_k are the proportion of the kth order mirror-like component in the total $R_{\rm s}$. Each term of (13) denotes different degree of specular reflectance component, which is more or less mirror-like. We think that the reflectance map $R_{\rm s}$ is composed by all different degrees of specular reflectance components. When used in practice, the finite terms of polynomial (13) can be shown as

$$R_{\rm s} = E\sum_{k=1}^{N}c_k(\vec{n}^{\rm T}*\vec{n}_{\rm spec})^k, \quad (14)$$

where N is associated with the most mirror-like component of $R_{\rm s}$. The characteristic of most practical object is hybrid, as described by the model (11) or the modified form (12). So a new polynomial hybrid reflectance model containing diffuse reflectance is brought forward as

$$R_{\text{hybrid}} = E[c_0\vec{n}^{\text{T}} * \vec{n}_{\text{i}} + \sum_{k=1}^{\infty} c_k(\vec{n}^{\text{T}} * \vec{n}_{\text{spec}})^k], \tag{15}$$

where c_0 can be considered as the proportion of diffuse component in the total R_{hybrid}. When the light strength E is merged with $c_1, c_2, \cdots, c_k$, Eq. (15) can be written as

$$R_{\text{hybrid}} = d_0\vec{n}^{\text{T}} * \vec{n}_{\text{i}} + \sum_{k=1}^{\infty} d_k(\vec{n}^{\text{T}} * \vec{n}_{\text{spec}})^k. \tag{16}$$

When used in practice, the finite terms of polynomial (16) can be shown as

$$R_{\text{hybrid}} = d_0\vec{n}^{\text{T}} * \vec{n}_{\text{i}} + \sum_{k=1}^{N} d_k(\vec{n}^{\text{T}} * \vec{n}_{\text{spec}})^k. \tag{17}$$

Once the reflectance model (17) is established, we will use a sample objective with known shape (denoted by its surface function, we select cylinder in our experiments) to determine the coefficients of (17) using the reflectance map function (5) by least square regression algorithm. Then the reflectance properties of the same class of materials can be obtained.

The reflectance model (17) is a function of $\vec{n}$, $\vec{n}_{\text{i}}$ and $\vec{n}_{\text{o}}$. The coefficients denote the reflectance properties. When the variables $\vec{n}$, $\vec{n}_{\text{i}}$ and $\vec{n}_{\text{o}}$ are known, the coefficients of $R_{\text{hybrid}}(\vec{n}, \vec{n}_{\text{i}}, \vec{n}_{\text{o}})$ can be acquired using least square regression algorithm. Assuming $\vec{n}_1$, $\vec{n}_2$, $\cdots$, $\vec{n}_M$ are M known directions of surface, from Eqs. (17) and (5), we get

$$\begin{bmatrix} I_1 \\ I_2 \\ \vdots \\ I_M \end{bmatrix} = \begin{bmatrix} (\vec{n}_1^{\text{T}} * \vec{n}_{\text{i}}) & (\vec{n}_1^{\text{T}} * \vec{n}_{\text{spec}})^1 & \cdots & (\vec{n}_1^{\text{T}} * \vec{n}_{\text{spec}})^N \\ (\vec{n}_2^{\text{T}} * \vec{n}_{\text{i}}) & (\vec{n}_2^{\text{T}} * \vec{n}_{spec})^1 & \cdots & (\vec{n}_2^{\text{T}} * \vec{n}_{\text{spec}})^N \\ \vdots & \vdots & \cdots & \vdots \\ (\vec{n}_M^{\text{T}} * \vec{n}_{\text{i}}) & (\vec{n}_M^{\text{T}} * \vec{n}_{\text{spec}})^1 & \cdots & (\vec{n}_M^{\text{T}} * \vec{n}_{\text{spec}})^N \end{bmatrix} \begin{bmatrix} d_0 \\ d_1 \\ \vdots \\ d_N \end{bmatrix}.$$

We write the above equation in matrix form as

$$\mathbf{I} = \mathbf{AD}. \tag{18}$$

In experiments, the number of image pixels M is larger than the highest order N of specular components. So Eq. (18) is an over-determined equation. The coefficients vector $\mathbf{D}$ is

$$\mathbf{D} = (\mathbf{A}^{\text{T}}\mathbf{A})^{-1}\mathbf{A}^{\text{T}}\mathbf{I}. \tag{19}$$

We also investigate a way to evaluate the performance of the proposed reflectance model and compare the image generated from reflectance maps (6), (10) and (17). Let $R_{(k)}$ denote the generated image, $I_{(k)}$ be the original image. The difference between them are the comparison criteria namely mean error (ME) and root square mean error (RS), which are defined as

$$\text{ME} = \frac{1}{M}\sum_{k=1}^{M} |R_{(k)} - I_{(k)}|, \tag{20}$$

$$\text{RS} = \sqrt{\frac{1}{M}\sum_{k=1}^{M} (R_{(k)} - I_{(k)})^2}. \tag{21}$$

Experiments are performed to evaluate the performance of the proposed model. Comparison results between the proposed model and existing ones are also shown. Figure 1 is a real acquired image of a metal cylinder. The light is located in 3-m distance. The diameter of the cylinder is 10 cm. We use camera center coordinates. In our experiments, parameters of the proposed model are acquired by the captured image of Fig. 1 and N is set as 20. Calculated $\{d_0, d_1, \cdots, d_{20}\}$ using (19) are {0.0895, 0.0239, 0.0362, 0.0441, 0.0485, 0.0426, 0.0375, 0.0316, 0.0253, 0.0189, 0.0153, 0.0200, 0.0298, 0.0348, 0.0400, 0.0453, 0.0562, 0.0674, 0.0788, 0.0847, 0.0905}. The generated images using proposed reflectance model, Phong model and Lambertian model are shown in Figs.2(a)—(c). Figure 3 shows the gray intensities of Figs. 2(a)—(c) along the surface directions (using cosine of their angles with axis of camera). Figure 4 shows the intensity errors of Figs. 2(a)—(c) compared with the intensity of the original surface of Fig. 1. Table 1 lists

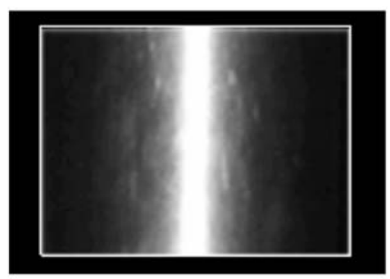

Fig. 1. Acquired image of a metal cylinder.

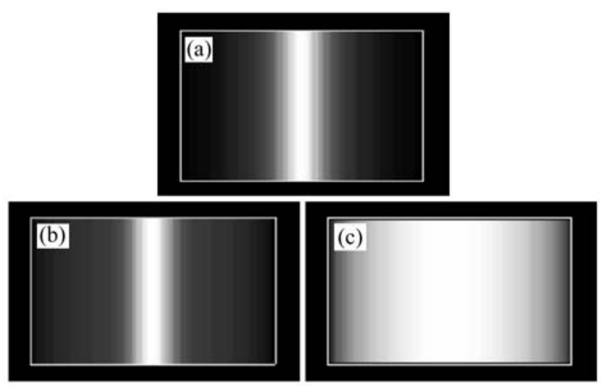

Fig. 2. Generated images using (a) the proposed model, (b) Phong model, and (c) Lambertian model.

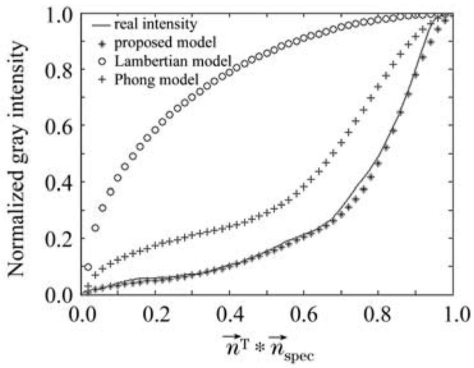

Fig. 3. Intensities of Figs. 2(a)—(c) along the surface directions.

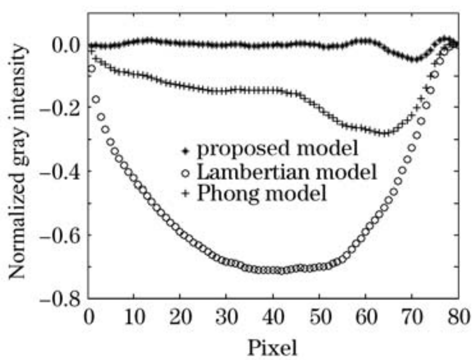

Fig. 4. Error of intensities compared with the original intensity of Fig. 1.

Table 1. Reflectance Maps of Three Models

	Proposed	Phong	Lambertian
ME	0.00439	0.15347	0.51338
RS	0.00153	0.01865	0.06172

the results using Eqs. (20) and (21). From the result, we can see that the proposed reflectance model is more accurate and flexible. It is suitable to describe the reflectance properties of real surface.

In conclusion, a new general polynomial hybrid reflectance model is proposed. We use the reflectance map equation with known shape to estimate the parameters of the proposed reflectance model by least square regression algorithm. Thus the reflectance properties of the same class of material can be determined. Experiments on real images show the proposed reflectance model is suitable for describing the real reflectance property. The proposed reflectance model may be used to deal with computer vision problems such as shape-from-shading with specular reflectance and improve the accuracy of three-dimensional (3D) reconstruction.

This work was supported by the National Natural Science Foundation of China under Grant No. 60502021. L. Yang's e-mail is yangyoungya@sina.com.

References

1. J. F. Blinn, Computer Graphics **11,** (2) 192 (1977).
2. S.-Y. Cho and T. W. S. Chow, Neural Computation **14,** 2751 (2002).
3. S. K. Nayar, K. Ikeuchi, and T. Kanade, IEEE Trans. Pattern Analysis and Machine Intelligence **13,** 611 (1991).
4. G. Bishop and D. M. Weimer, Computer Graphics **20,** (4) 103 (1986).
5. G. J. Ward, Computer Graphics **26,** (2) 265 (1992).
6. K. M. Lee and C.-C. J. Kuo, Computer Vision and Image Understanding **67,** 143 (1997).
7. Q. Zheng and R. Chellappa, IEEE Trans. Pattern Analysis and Machine Intelligence **13,** 680 (1991).
8. S.-Y. Cho and T. W. S. Chow, IEEE Trans. Neural Networks **11,** 1498 (2000).
9. H. D. Tagare and R. J. P. deFigueiredo, IEEE Trans. Pattern Analysis and Machine Intelligence **13,** 133 (1991).
10. C.-T. Lin, W.-C. Cheng, and S.-F. Liang, IEEE Trans. Neural Networks **16,** 1601 (2005).
11. X. Wu, D. Guo, and X. Wang, Computer Engineering and Applications (in Chinese) **24,** (19) 23 (2001).
12. S. R. Marschner, S. H. Westin, E. P. F. Lafortune, and K. E. Torrance, Appl. Opt. **39,** 2592 (2000).
13. R. Basri and D. W. Jacobs, IEEE Trans. Pattern Analysis and Machine Intelligence **25,** 218 (2003).
14. P. Lalonde and A. Fournier, IEEE Trans. Visualization and Computer Graphics **3,** 329 (1997).
15. W. Matusik, H. Pfister, M. Brand, and L. McMillan, ACM Trans. Graphics **22,** 759 (2003).
16. R. Zhang, P.-S. Tsai, J. E. Cryer, and M. Shah, IEEE Trans. Pattern Analysis and Machine Intelligence **21,** 690 (1999).
17. L. Yang and J. Han, Chin. Opt. Lett. **5,** 204 (2007).
18. B. T. Phong, Communications of the ACM **18,** 311 (1975).